Journal of Power Sources 195 (2010) 522–526

Contents lists available at ScienceDirect

Journal of Power Sources

journal homepage: www.elsevier.com/locate/jpowsour

Short communication

Electrical behavior of aluminosilicate glass-ceramic sealants and their interaction with metallic solid oxide fuel cell interconnects

Ashutosh Goel, Dilshat U. Tulyaganov, Vladislav V. Kharton, Aleksey A. Yaremchenko, José M.F. Ferreira*

Department of Ceramics and Glass Engineering, University of Aveiro, CICECO, 3810-193 Aveiro, Portugal

ARTICLE INFO

Article history:
Received 19 May 2009
Received in revised form 19 July 2009
Accepted 6 August 2009
Available online 14 August 2009

Keywords:
Glass-ceramic sealants
Solid oxide fuel cell (SOFC)
Diopside
Electrical properties
Chemical interaction
Interconnect

ABSTRACT

A series of alkaline-earth aluminosilicate glass-ceramics (GCs) were appraised with respect to their suitability as sealants for solid oxide fuel cells (SOFCs). The parent composition with general formula $Ca_{0.9}MgAl_{0.1}La_{0.1}Si_{1.9}O_6$ was modified with Cr_2O_3 and BaO. The addition of BaO led to a substantial decrease in the total electrical conductivity of the GCs, thus improving their insulating properties. BaO-containing GCs exhibited higher coefficient of thermal expansion (CTE) in comparison to BaO-free GCs. An extensive segregation of oxides of Ti and Mn, components of the Crofer22 APU interconnect alloy, along with negligible formation of $BaCrO_4$ was observed at the interface between GC/interconnects diffusion couples. Thermal shock resistance and gas-tightness of GC sealants in contact with yttria-stabilized zirconia electrolyte (8YSZ) was evaluated in air and water. Good matching of CTE and strong, but not reactive, adhesion to the solid electrolyte and interconnect, in conjunction with a high level of electrical resistivity, are all advantageous for potential SOFC applications.

© 2009 Elsevier B.V. All rights reserved.

1. Introduction

The most arduous task in the commercialization of planar SOFC is the hermetic sealing provided to its ceramic and metallic components such that the resulting joints remain rugged and stable over the lifetime of the stack. The seals must have CTE similar to those of other cell components $(9–12) \times 10^{-6}\,K^{-1}$; be stable in a wide range of oxygen partial pressure (air and fuel) and be chemically compatible with other fuel cell (FC) components, while minimizing thermal stresses during high-temperature operation which creates a major challenge in the development of planar SOFCs. Substantial work is in progress in this area, aimed at improving the performance of sealants under extreme operating conditions of current fuel cell designs, which involve both high temperatures and highly corrosive environments. Also, a compliant sealant is expected to behave as an electrical insulator, with total conductivity lower than $10^{-4}\,Scm^{-1}$, in order to avoid parasitic currents decreasing the system's efficiency [1,2]. Among the various concepts of sealing proposed so far [2,3], GCs have emerged to be the most promising candidates [4]. However, most of the GC based sealants proposed so far have some advantages which are coupled along with some drawbacks. Therefore, still there is a need to fill in this lacuna by developing a suitable sealing material for SOFC technology.

Recently, La_2O_3-containing alkaline-earth aluminosilicate diopside based GC sealants with very low amounts of BaO and B_2O_3 have been proposed [5,6]. However, some adverse reactions were observed at the interface between GC sealant and metallic interconnect leading to the formation of barium–chromium rich oxides. Also, still there is need to increase and stabilize the CTE of the diopside based GC sealants during long term heat treatment and to improve the flow behavior of the resultant GCs in order to qualify those for the applications in SOFC stack. Thus, in the light of above mentioned perspective, the present study is an attempt to design new GC sealants in order to tailor their CTE and reduce adverse chemical reactivity with metallic interconnect without compromising with their electrical and joining properties, so as to fulfill the criteria of a compliant sealing material required for SOFCs.

A new series of alkaline-earth aluminosilicate glasses were prepared by modifying the parent composition with general formula $Ca_{0.9}MgAl_{0.1}La_{0.1}Si_{1.9}O_6$. Table 1 lists the glass compositions. The first glass (labeled as 10) was derived by adding 2 wt.% B_2O_3 to the glass composition $Ca_{0.9}MgAl_{0.1}La_{0.1}Si_{1.9}O_6$. The second glass (10A) was followed by addition of 0.5 wt.% Cr_2O_3 to composition 10. It is well documented that addition of Cr_2O_3 decreases the crystallization temperature [6] and reduces surface tension [7] of the glasses. Also, the presence of Cr_2O_3 in the glasses may help in suppressing the diffusion of Cr from metallic interconnects into the bulk of GC sealant, thus, preventing massive formation of $BaCrO_4$ and other barium–chromium oxide compounds having detrimental impact in air. The remaining three glasses, i.e. 10B, 10C and 10D were derived

* Corresponding author. Tel.: +351 234 370242; fax: +351 234 370204.
E-mail address: jmf@ua.pt (J.M.F. Ferreira).

0378-7753/$ – see front matter © 2009 Elsevier B.V. All rights reserved.
doi:10.1016/j.jpowsour.2009.08.007

Table 1
Batch compositions of the glasses (wt.%).

Glass	MgO	CaO	BaO	SiO_2	Al_2O_3	La_2O_3	B_2O_3	Cr_2O_3	NiO
10	17.27	21.63	–	48.93	2.18	6.98	2	–	1
10A	17.19	21.52	–	48.67	2.17	6.95	2	0.5	1
10B	16.48	18.34	6.27	46.67	2.08	6.66	2	0.5	1
10C	16.14	16.85	9.21	45.73	2.04	6.53	2	0.5	1
10D	15.83	15.41	12.04	44.82	2.00	6.40	2	0.5	1
7-2B [5]	16.56	18.44	6.30	46.91	2.09	6.70	2	–	1

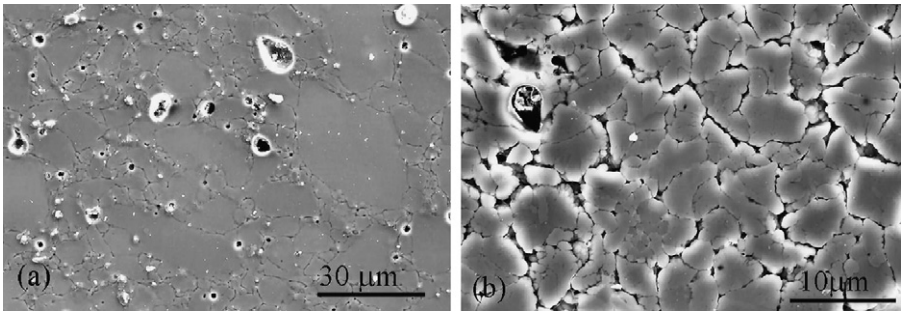

Fig. 1. SEM image of glass-powder compacts from composition (a) 10B heat treated at 800 °C and (b) 10C heat treated at 850 °C for 1 h.

by partial substitution of CaO by BaO in the glass composition 10A. The composition for glass 7-2B is listed in Table 1 for comparison purposes [5]. It is noteworthy that the amount of BaO and B_2O_3 in the investigated glasses is significantly lower in comparison to other sealants proposed in literature [2]. Therefore; negligible seal degradation can be expected.

2. Experimental

All the investigated glasses were prepared in bulk and frit form by melt-quenching technique. A detailed description of the experimental section pertaining to preparation of glasses and GCs has been described in our previous studies [6]. The glass-powder compacts were sintered under non-isothermal conditions for 1 h at 800 °C and 850 °C. A slow heating rate of 2 K min^{-1} was maintained in order to prevent deformation of the samples. Further, rectangular bars already sintered at 850 °C, were heat treated under isothermal conditions at 800 °C for 300 h. The amorphous nature of the glasses and crystalline phase evolution in GCs was followed by X-ray diffraction (XRD) and scanning electron microscopy (SEM) analysis while dilatometer was employed in order to measure the CTE of the GCs, as depicted in Ref. [5]. The measurement of total conductivity of GCs by AC impedance spectroscopy is detailed in Ref. [5]. The ion transference numbers were assessed by the modified electromotive-force (e.m.f.) technique, as described in Ref. [8].

The experimental description for investigating adhesion and chemical interaction of GCs with 8 mol.% yttria-stabilized zirconia (8YSZ, Tosoh, Japan) and Crofer22 APU (Thyssen Krupp, VDM, Werdohl, Germany) after 300 h of heat treatment at SOFC operating temperature along with thermal shock resistance of GC sealants when in contact with 8YSZ has been described in our previous study [5]. In order to evaluate thermal shock resistance of the GC sealants in contact with stabilized zirconia electrolyte, a series of model cells were made by sealing dense 8YSZ tubes onto 8YSZ disks. Hermetic sealing was performed using powdered GCs, with final annealing at 1275 °C for 0.5 h. Then each pseudo-cell was heated in the furnace up to 800 °C, kept at this temperature for 0.5 h, and quenched in air or in water. After subsequent checking of the gas-tightness, each cell was rapidly heated again, and the quenching cycle was repeated. The 8YSZ pseudo-cells were successfully tested in 15 air-quenching cycles.

3. Results and discussion

For all the investigated compositions (Table 1), melting at 1550 °C for 1 h was adequate to obtain bubble-free, amorphous transparent glasses. The structural, physical and thermal properties of the parent glasses are out of the scope of this paper and will be published in forthcoming article.

The heat treatment of glass-powder compacts at 800 °C for 1 h resulted in well-sintered but amorphous bodies as was confirmed by XRD and SEM studies (Fig. 1a). Augite ($Ca(Mg_{0.85}Al_{0.15})((Si_{1.70}Al_{0.30})O_6$; ICDD card: 01-078-1391) crystallized in all the GCs after heat treatment at 850 °C (Fig. 1b and 2a). The CTE (200–600 °C) values of the GCs sintered at 850 °C for 1 h are presented in Table 2. Since, the amorphous phase in the GCs plays a crucial role in deciding the reaction kinetics between GC sealant and SOFC components; therefore, it is essential to quantify the amount of crystalline and amorphous phase in the GC sealants. This point shall be focused upon it in our further publication. The CTE values decreased with addition of Cr_2O_3 while increased with an increase in BaO content in the glasses until composition 10C. However, with further replacement of CaO by BaO in composition 10D, the CTE decreased considerably. The highest CTE value for the GCs was observed for composition 10C (9.5×10^{-6} K^{-1}) while the lowest was observed for composition 10D (8.8×10^{-6} K^{-1}).

The crystalline phase evolution after prolonged heat treatment of GCs (already sintered at 850 °C for 1 h) at 800 °C for 300 h is presented in Fig. 2b. Augite crystallized as the only phase in GC 10 and 10A while hexacelsian (HC; $BaAl_2Si_2O_8$; ICDD: 01-088-1048) appeared as secondary phase along with augite in GC 10B and 10C. The intensity of XRD peaks was lower for all the investigated GCs after 300 h of heat treatment in comparison to GC sintered at 850 °C for 1 h. After heat treatment of 300 h, the

Table 2
CTE × 10^6 K^{-1} (200–600 °C) of the GCs produced at different conditions.

Composition	850 °C, 1 h	800 °C, 300 h
10	9.2	8.8
10A	9.1	9.0
10B	9.4	9.2
10C	9.5	9.2
10D	8.8	9.0

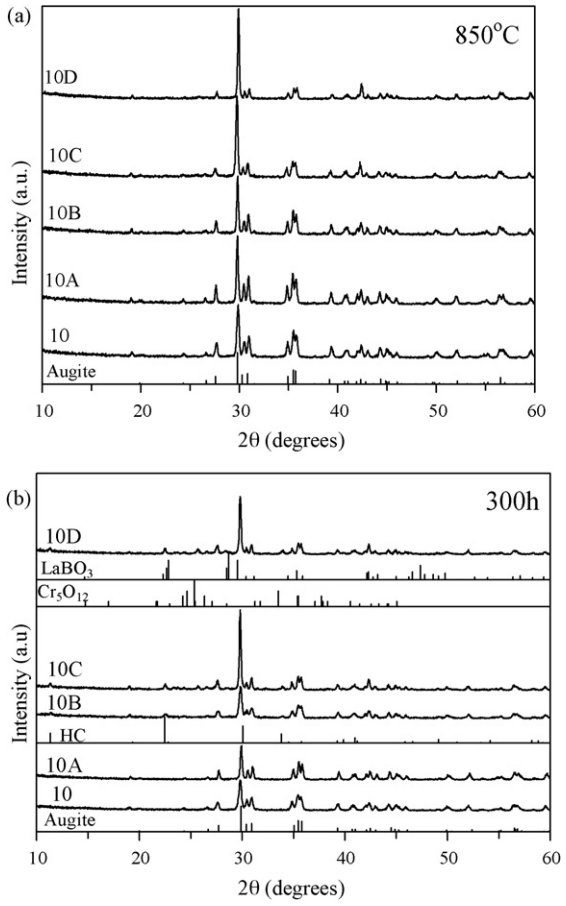

Fig. 2. X-ray diffractograms of glass-powder compacts sintered at (a) 850 °C for 1 h, (b) 850 °C for 1 h followed by 800 °C for 300 h.

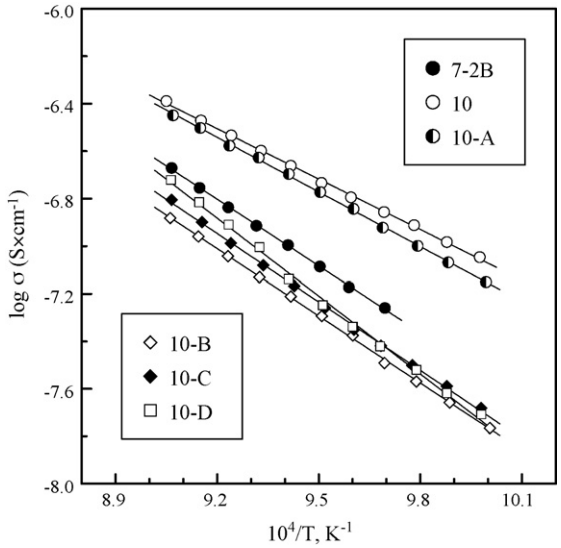

Fig. 3. Total conductivity of dense GCs in air. The data on 7-2B [5] are shown for comparison. The error bars are smaller than the data point symbols.

intensity of XRD peaks for GCs 10 and 10A was almost similar while GC 10C showed the XRD peaks with highest intensity implying towards higher crystallinity. In GC 10D, two more minor phases, namely, $LaBO_3$ (ICDD: 00-013-0571) and a solid solution isostructural to Cr_5O_{12} (ICDD: 00-018-0390) crystallized out along with augite and HC. Similar crystalline phase ($LaBO_3$) was also observed by Mahapatra et al. [9] during devitrification of $(25-X)SrO–20La_2O_3–(7+X)Al_2O_3–40B_2O_3–8SiO_2$ (mol%), where $X = 0–10$ mol.% and explained it on the basis of tendency of La^{3+} to coordinate with triangular coordinated boron due to the high electrostatic bond strength of the former. In the present investigation, this phase was observed only for the GC with highest amount of BaO (10D).

The CTE (200–600 °C) values for the GCs heat treated at 800 °C for 300 h are presented in Table 2. The CTE values for all the GCs decreased after prolonged heat treatment in comparison to the parent GC compositions (sintered at 850 °C for 1 h) due to the decrease in crystallinity of the GCs. In accordance with the results obtained for parent GCs, the CTE values increased with an increase in BaO content until composition 10C. The highest CTE was obtained for GC 10C ($9.2 \times 10^{-6}\,K^{-1}$) while the lowest were obtained for GCs 10A ($9.0 \times 10^{-6}\,K^{-1}$) and 10D ($9.0 \times 10^{-6}\,K^{-1}$), respectively.

The results of impedance spectroscopy (Fig. 3) confirmed excellent insulating properties of the GC materials in spite of the conductivity increase caused by B_2O_3 addition as reported in our previous work [5]. At 830 °C, the maximum conductivity observed in the studied system for the parent composition, Glass 10, is as low as 4×10^{-7} Scm^{-1}. This level ensures an absence of short circuiting between the SOFC stack components, especially in the intermediate temperature range. Barium additions lead to a substantial decrease in the total conductivity and to an increase of the corresponding activation energy calculated by the standard Arrhenius equation (Table 3). At temperatures below 780–800 °C, the conductivity of all Ba-containing GCs (10B, 10C and 10D) becomes similar within the limits of experimental uncertainty. Testing of the GCs in humidified air atmosphere confirmed that water incorporation can be neglected as no conductivity changes were observed within the limits of experimental error. Assessment of the conductivity mechanisms by the modified e.m.f. method under air/10%H_2–90%N_2 gradient displayed a predominantly ionic transport; the ion transference numbers are higher than 0.93, as for the parent systems [6]. Possible mechanisms were discussed elsewhere [6,8].

Fig. 4 presents the SEM micrograph of GC 10B-8YSZ pseudo-cell after thermal shock experiments in air. No cracks development in the GCs was observed; sealing remained gas-tight, demonstrating an excellent thermal shock resistance and, thus, suitability of the GC sealants for any startup/shutdown protocols in SOFCs. The quenching in water resulted, however, in embrittlement and cracking of the GCs.

All the sealing GCs bonded well to the metallic interconnect and no gaps were observed even at the edges of the joints. Fig. 5a shows SEM image of the interface of Crofer22 APU/glass 10 join after heat treatment at 850 °C for 1 h, followed by 800 °C for 300 h in air. A rather smooth interface between GC 10 and Crofer22 APU was observed without the presence of iron-rich oxide products. Also, the formation of Mn, Cr-rich oxides could not be seen at the interface (Fig. 5b). However, presence of a Ti-rich zone near the interface was the main feature that was observed in all the diffusion couples between GCs (10, 10A, 10B, 10C) and Crofer22 APU except GC 10D/Crofer22 APU diffusion couple (Figs. 5 and 6).

Table 3
Activation energy for the total conductivity (730–830 °C) of GCs in air.

Glass	E_A (kJ mol^{-1})
7-2B [5]	188 ± 4
10	144 ± 3
10A	156 ± 3
10B	189 ± 3
10C	192 ± 4
10D	218 ± 8

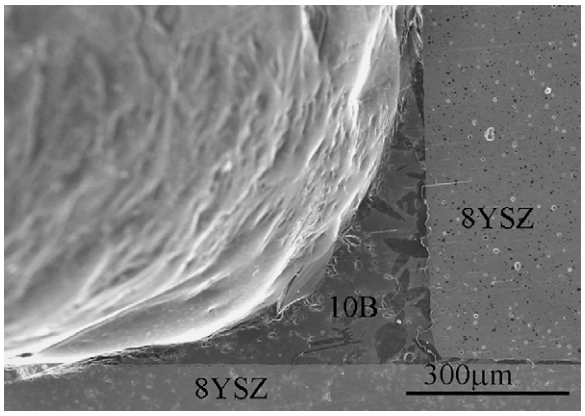

Fig. 4. SEM image of the 8YSZ-GC 10B pseudo-cell after thermal shock resistance experiments in air after 15 quenching cycles.

This formation of titanium oxide layer may have several positive effects; first of all, since the outer layer contains no Cr, the migration of Cr to the cathode which poisons its effectiveness would be expected to be greatly reduced if not eliminated [10,11]. A similar observation was reported by Jablonski and Alman [12] for a steel containing 22 wt.% Cr and 1 wt.% Ti when surface treated by CeO_2 while untreated steel samples did not show formation of Ti-enriched protecting layers. According to Jablonski and Alman [12], the formation of titanium oxides is much more favorable from

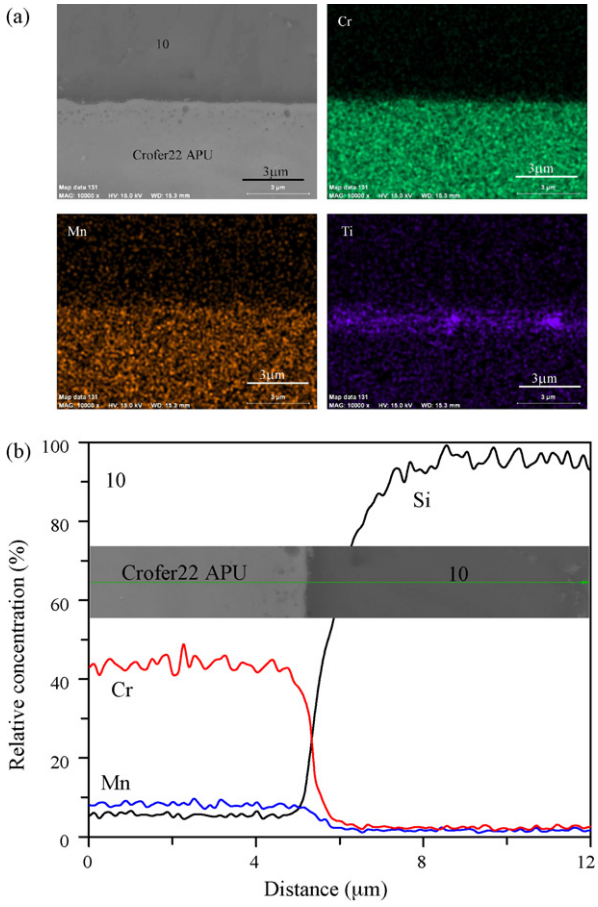

Fig. 5. (a) Microstructure (SEM) and EDS element mapping of Cr, Mn, and Ti and (b) EDS line profile for diffusion of Cr, Mn and Si at interface between GC 10 and Crofer22 APU developed after heat treatment at 850 °C for 1 h and 800 °C for 300 h in air.

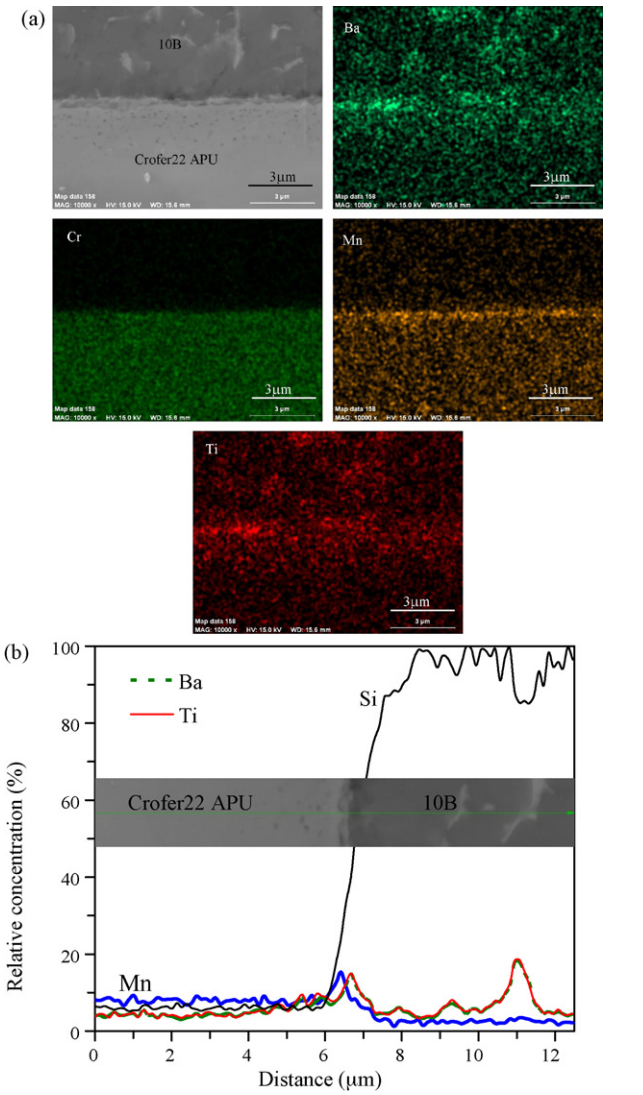

Fig. 6. (a) Microstructure (SEM) and EDS element mapping of Ba, Cr, Mn and Ti at the interface between GC 10B and Crofer22 APU (b) EDS line profile for diffusion of Ba, Cr, Mn and Ti from GC 10B to Crofer22 APU and vice versa at their interface developed after heat treatment at 850 °C for 1 h and 800 °C for 300 h in air.

thermodynamic point of view, in comparison to the other Cr, Mn-rich oxidizing species. Further, as is evident from Fig. 6a and b, substantial segregation of manganese takes place along with Ti at the oxidized interface of diffusion couple between GC 10B (also for GC 10C) and metallic interconnect. These results may indicate towards the (a) possible formation of Mn-rich oxides along with titanium oxide or (b) formation of Mn, Ti-oxides. Since, the standard Gibbs energy for formation of Mn, Ti-oxides at 800 °C (for example: $MnTiO_3$ = 298 kJ mol^{-1}, Mn_2TiO_4 = 276 kJ mol^{-1}) is significantly higher than Mn-oxides (for example: MnO = 217 kJ mol^{-1}, MnO_2 = 208 kJ mol^{-1}, Mn_2O_3 = 221 kJ mol^{-1}, Mn_3O_4 = 224 kJ mol^{-1}) [12], possible formation of the former seems to be more feasible in reducing atmospheres where Mn^{2+} cations exist; in air, when Mn^{3+} and Mn^{4+} oxidation states prevail, formation of binary oxides mixture is more likely. Another feature to be noted is that Ba rich zones could be observed while no Cr-rich zones were found along the interface of the diffusion couples. The EDS element profile (Fig. 6b) depicts the occurrence of Ba along with Ti at the interface pinpointing towards the possible formation of a $BaTiO_3$ based solid solution. $BaTiO_3$ is a relatively stable phase with respect to the redox behavior and thermo-mechanical properties,

and should have no detrimental impact on the SOFC performance. No Cr-rich zones could be seen all along the interface, therefore, occurrence of any adverse reaction between Ba and Cr could be neglected which is, again, highly favorable for sealing application. With an increase in BaO content (GC 10D), a thin zone rich in Cr and Mn was observed at the interface between GC 10D and Crofer22 APU implying towards the formation of Mn, Cr-spinel while no adverse reactions were observed between BaO and Cr_2O_3.

4. Conclusions

Well-sintered GCs with augite as the primary crystalline phase were obtained in all the compositions. The addition of BaO led to a progressive decrease in the total conductivity of the GCs and to progressive increase of the activation energies, thus, ensuring an absence of short circuiting between the SOFC stack components, especially in the intermediate temperature range. The addition of BaO increased the CTE of the resultant GCs which showed high thermal stability during long term heat treatments. The investigated GC sealants, 10B and 10C, demonstrated a good thermal shock resistance in air while cracks were only developed on quenching in water. Formation of Ti-rich oxide layers at the interface between GC sealants and Crofer22 APU was observed while no adverse reactions leading to the formation of $BaCrO_4$ were observed in any of the investigated diffusion couples.

Acknowledgement

This study was financially supported by University of Aveiro, CICECO and FCT, Portugal (SFRH/BD/37037/2007).

References

[1] S.P.S. Badwal, K. Foger, Ceram. Int. 22 (1996) 257.
[2] J.W. Fergus, J. Power Sources 147 (2005) 46.
[3] K.S. Weil, C.A. Coyle, J.S. Hardy, J.Y. Kim, G.-G. Xia, Fuel Cells Bull. (2004) 11.
[4] I.W. Donald, B.L. Metcalfe, L.A. Gerrard, J. Am. Ceram. Soc. 91 (2008) 715.
[5] A. Goel, D.U. Tulyaganov, V.V. Kharton, A.A. Yaremmchenko, S. Eriksson, J.M.F. Ferreira, J. Power Sources 189 (2009) 1032.
[6] A. Goel, D.U. Tulyaganov, V.V. Kharton, A.A. Yaremchenko, J.M.F. Ferreira, Acta Mater. 56 (2008) 3065.
[7] T. Schwickert, R. Sievering, P. Geasee, R. Conradt, Mat. Wiss. Werkst. 33 (2002) 363.
[8] A. Goel, D.U. Tulyaganov, V.V. Kharton, A.A. Yaremchenko, S. Agathopoulos, J.M.F. Ferreira, J. Am. Ceram. Soc. 90 (2007) 2236.
[9] M.K. Mahapatra, K. Lu, W.T. Reynolds Jr., J. Power Sources 179 (2008) 106.
[10] Z. Yang, G. Xia, P. Singh, J.W. Stevenson, J. Power Sources 155 (2006) 246.
[11] X. Chen, P.Y. Hou, C.P. Jacobson, S.J. Visco, L.C. De Jonghe, Solid State Ionics 176 (2005) 425.
[12] P.D. Jablonski, D.E. Alman, J. Power Sources 180 (2008) 433.